

## IAC-04-I.4.10

# LIGHTWEIGHT DEPLOYABLE BOOMS: DESIGN, MANUFACTURE, VERIFICATION, AND SMART MATERIALS APPLICATION

C. Sickinger,

*christoph.sickinger@dlr.de,*

L. Herbeck, T. Ströhlein, J. Torrez-Torres

*lars.herbeck@dlr.de, tobias.stroehlein@dlr.de, jorge.torrez-torres@dlr.de*

*German Aerospace Center (DLR e. V.)*

*Institute of Structural Mechanics*

*Lilienthalplatz 7, D-38108 Brunswick, Germany*

**Abstract:** *Large and ultra-light space structures on base of deployable components will gain in importance for a row of future mission applications. The DLR Institute of Structural Mechanics is developing deployment concepts for ultra-light carbon-fibre reinforced struts (CFRP booms), which can be coiled around a hub for stowage within a very tight transportation volume. The development of cost-efficient and qualified production technologies for considerably long booms as well as the design verification including on-ground deployment tests are further tasks currently being worked out. Adaptive materials are efficient means to reduce the oscillations of the very large and flexible structures. They were successfully development tested and demonstrated in the framework of a boom test campaign on shortened samples. The deployable CFRP boom design is applied to a joint ESA/DLR Solar Sail in-orbit demonstration project. Four 14 meter long booms are designed, manufactured, verified, and finally integrated. The specific mass of the booms amounts to only 100 grams per meter for this application.*

### INTRODUCTION

Deployable space structures play traditionally an important part in the realization of space missions since the limited envelopes of the existing launchers constrain the payloads geometrically. Increasing demands, for example for energy supply, require more and more very large appendages. Power generation of the International Space Station (ISS) is provided by eight deployable solar arrays, each spreading an area of approximately 32.6 m to 11.6 m. The 60 m long boom which was deployed and retracted in 2000 on board of the Space Shuttle Endeavour during the Shuttle Radar Topography Mission (SRTM) is another prominent example. Presently, a clear trend for an increasing need can be identified for a number of future space structure applications like instrument booms, antennas and reflectors, Solar Sails, and huge solar power systems. European space industries are increasingly harmonized by ESA's European Space Technology Master Plan (ESTMP). The need for key technologies is identified and development activities are envisaged to be supported by the establishment of research programs. In 2000, for example, solar arrays and synthetic-aperture radar (SAR) technologies were harmonized [1]. Both are potential fields of application for deployable structures and the initiation of the harmonization of inflatable systems and deployable booms in 2003 clearly indicate the

increasing need for deployable space structures development. Consequently, ESA and DLR are developing in a common effort important key technologies in a Solar Sail in-orbit demonstration. The extreme requirements connected to that specific project stand representatively for a number of engineering challenges in the field of deployable space structures. The DLR Institute of Structural Mechanics contributes an assembly of four deployable ultra-light carbon-fibre reinforced booms to the Solar Sail project. In its expanded configuration the boom assembly provides the supporting structure for the tightening of the flexible sail membrane.

### DESIGN AND ANALYSIS

In the design of the deployable boom assembly, each of the booms can be pressed down flatly and rolled around a spool for stowage within a very small transportation volume. Ultra-thin prepregs made of carbon-fibre reinforced plastics (CFRP) are used for the manufacture of the booms. They are cured to two half cross-sections and subsequently bonded together at the even bonding flanges. The laminate setup is made up of a combination of 0°- and  $\pm 45^\circ$  layers. In addition to a favorable influence on the buckling behavior of the very thin-walled structure, the choice of the stacking sequence is essentially based on the requirement to minimize the bending that



Fig. 1: Deployable CFRP boom. Length 14 m, mass 1.4 kg.

takes place during single-sided thermal loading as it will be expected if the booms are exposed to the radiation environment in space. For this reason, a very low coefficient of thermal expansion (CTE) in the boom longitudinal direction is an important prerequisite ( $CTE_1 \approx 0 K^{-1}$ ). The structural boom design is based on requirements that were determined during a Solar Sail ground demonstration [2]. Although only 14-meter long booms were built during this demonstration phase, the design was worked out according to future mission applications for a length of 28 meters. The cross-section geometry definition results from a mass optimization while fulfilling a certain minimum bending stiffness requirement and geometrical constraints. Finally, the specific mass of the booms amounts to 100 grams per meter only. Following the lightweight philosophy of the boom design, the internal energy of the booms, which is stored during the packaging procedure, can also be used for the deployment. The self-deployment test depicted in Figure 2 — completely driven by elastic deformation energy — takes only 10 seconds. However, a controlled and guided deployment or a retraction of the boom require therefore special mechanisms. For the Solar Sail application a deployment module is developed, which contains and latches the boom assembly in stowed configuration and guides the deployment sequence.

The demand for an ultra-light Gossamer structure inevitably leads to a membrane-like, thin-walled structure that has an extremely large surface in relation to its volume and, as a result, has an intensive exchange of radiation with its environment. Minimum and maximum tempera-

tures, thermal gradients in the boom cross-section, and transient events such as the shadowing of sub-systems or the Earth eclipse therefore have to be particularly taken into consideration during the boom design and material selection process. Figure 3 depicts the computed transient temperature distribution of the boom's flange section for a thermal load case of solar and terrestrial radiation at low Earth orbit. Coating measures that positively influence the thermal budget of the CFRP booms and that also provide protection against additional space environment conditions such as atomic oxygen have already been successfully examined in development tests (Fig. 8).



Fig. 2: The internal deformation energy of a stowed boom package enables the self-deployment of the 14 m long boom.

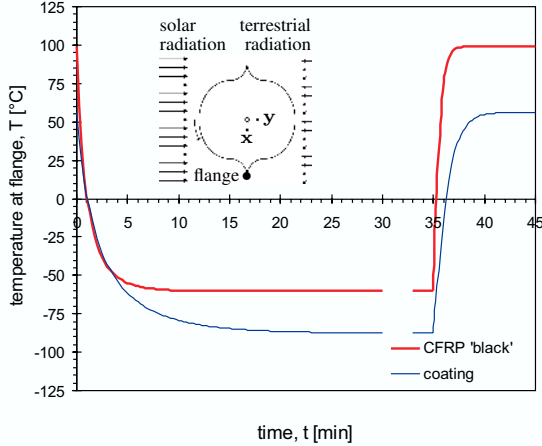


Fig. 3: Transient thermal computation of a coated and un-coated boom cross-section at Earth orbit. Flange temperature as a function of a transient event (Earth eclipse).

The modified thermo-optical properties clearly reduce the thermal gradients of the temperature distribution around the cross-section as well as thermal shocks.

Because of the role it plays in the entire concept, the structural design of the booms is very significant. Stiffness restrictions, such as those in the form of minimum bending stiffness requirements, as well as strength requirements are usually defined. From a global point of view, the booms can be described by defining the beam stiffness  $EI_x$ ,  $EI_y$ ,  $GJ_z$  and  $EA$  with an uniaxial beam model. The loading limit, on the other hand, is characterized in the thin-walled profile only by the buckling stability that, as an essential part of the structural description, has to be analyzed in detail.

Highly nonlinear Finite Element (FE) computations are applied to the analysis of the boom stability behavior. The result of the buckling analysis for the load case of an uniaxial bending  $M_x$  is depicted in Figure 4 in the form of a load-displacement curve. First, a computation of the linear static solution is made to get information on the nominal boom stiffness in a simple manner. A linear eigenvalue buckling analysis is performed afterwards. The computation of the eigenvalues and eigenvectors are used to define reasonable load ranges for the subsequent nonlinear computation. The eigenvectors are additionally used to define the geometrical imperfections that are necessary to initiate the nonlinear solution. In this case the first two eigenforms are analyzed and applied to the FE mesh with a maximum imperfection amplitude to the size of the boom's wall thickness. In addition to that, a single buckle imperfection at the most compression-loaded node of the cross-section is considered as well. In opposite to load case  $M_y$ , snap-through buckling suddenly occurs on the post-buckling curve while forming a typical diamond-shaped buckling pattern. The corresponding load level is so low that the stability and strength limits of

the boom are identical in case of a force-controlled loading.

The buckling limits of thin-walled shell structures react generally very sensitive to imperfections. Therefore, the boom design verification is also worked out at a very early stage of the development by engineering testing and not by analysis only. On the other hand, structural tests, particularly those which must be conducted to examine ultra-light deployables, are expensive and partially impracticable under one-g environment without exhaustive efforts. Verification by analysis plays therefore more and more an important role in the engineering domain for deployable structures. The traditional application of factors of safety (FoS) usually requires a sufficient amount of experiences with comparable exercises. A particular sensitive phenomenon could be otherwise underestimated even though a conservative assumption is applied. In case of the boom design, unnecessary conservatism, however, would dissatisfy the lightweight philosophy. New and innovative designs, such as those presented here, normally do not offer reliable information on past experiences. For

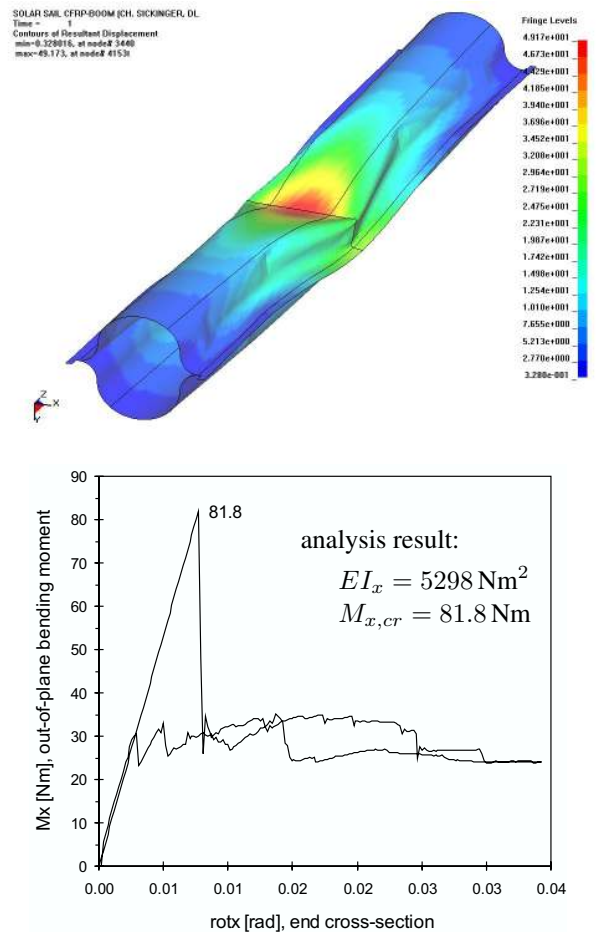


Fig. 4: Explicit Finite Element analysis of the buckling behavior according to uniaxial bending  $M_x$ .

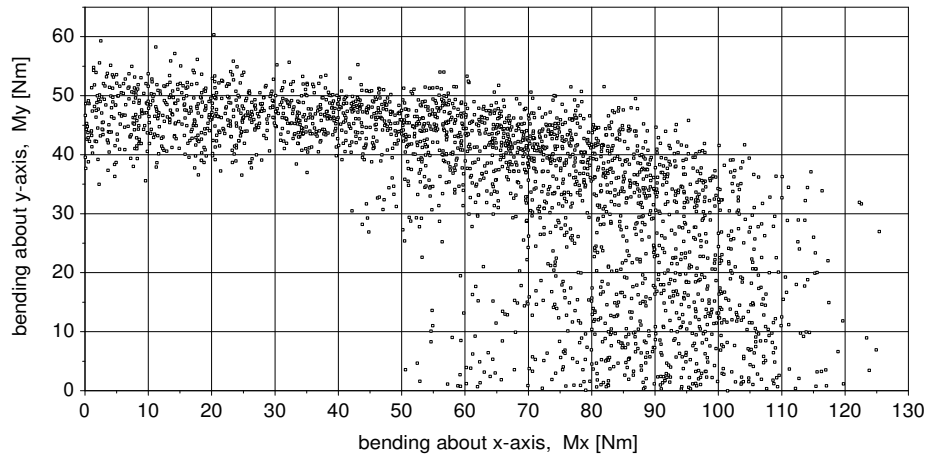


Fig. 5: Probabilistic buckling analysis of the boom strength. Monte-Carlo simulation with 2500 random samples. Stochastic population as a base for the development of a boom failure criterion.

this reason, the tracking of the scatter of design variables is an interesting alternative to the traditional deterministic way of structural design. The parameter scattering can be considered by use of a probabilistic Monte-Carlo simulation. Significant design variables are defined by certain stochastic distribution functions and the subsequent analysis results in probabilistic output variables. The following parameters are taken into consideration for the determination of the probabilistic boom stiffness and buckling limits:

- varying shell wall thicknesses as the result of a variation of the fibre areal weight of the carbon-fibre prepregs,
- CFRP material data depending on the prepreg lay-up accuracy of every single layer including the correlation of the laminate stiffness, for example the Young's modulus  $E_1$  to  $E_2$ ,
- geometrical manufacturing tolerances of the boom cross-section,
- geometrical imperfection amplitudes of the three imperfection modes for the nonlinear calculation of the buckling load,
- load eccentricities as the result of a cross-section distortion due to the nominal loading direction.

The Monte Carlo simulation is carried out via the computation of the nonlinear loading until the bifurcation point is met by use of an implicit FE code. The result is depicted in Figure 5 for the boom bending. Since the input parameters are defined stochastically the analysis output is no longer deterministic but probabilistic as well. Reliability investigations become possible and sensitivity plots give information on the correlation between certain

input parameters and the statistic result. Design improvements can therefore be initiated much more goal-directed.

The probabilistic computations, however, clearly follow another objective as well. From the system analysis side, it is not very efficient to model the sub-system boom assembly in detail with shell elements. On the other hand, if the local buckling behavior is not considered by a simplified uniaxial beam formulation, it will not be possible to simply make a statement on the boom failure under any system loads or to carry out lightweight system optimizations. The detailed probabilistic boom computations can therefore be used to establish a boom failure mode criterion based on the uniaxial beam load at boom assembly sub-system level. This criterion is then made available for a system analysis and allows for the computation of the safety margins at a general load. The development of a boom failure criterion on base of probabilistic simulations is reported in [7] and the evaluation of this criterion at a certain Solar Sail load case is depicted in Figure 17.

#### MANUFACTURE AND PRODUCTION

To manufacture the CFRP boom half-shells prepreg technology is used. This is essential to meet all requirements of the material and laminate quality and the small thicknesses which are necessary for the realization of the boom design. By performing a standard prepreg-process, fiber-layers, which are pre-impregnated with resin, are laid into a mold and subsequently evacuated and compressed by a vacuum-bag. The curing process is normally carried out inside an autoclave in compliance with the temperature cycles and pressurization required for the necessary laminate quality.

While producing the ultra-thin CFRP half-shells some more quality items must be taken into account beside the



Fig. 6: Production facilities: modular CFRP tooling and bake-out tent for vacuum-bagging and low-cost boom manufacturing.

well-known prepreg quality assurance parameters. With regard to the large boom length, the tool must be compatible to the coefficients of thermal expansion of the laminate. Therefore, the tools are made of CFRP as well. They are designed to have the same lay-up and equivalent fibers embedded as the laminate of the boom half-shells. A resin infusion technique, so-called Single-Line Injection (SLI) which was developed at the DLR, is used to manufacture the tools. Each of the molds is built up modularly from approximately 2.4 m long segments. The modular design allows the simple realization of different tool lengths. However, such a concept entails the exact alignment and clamping of the individual segments and also a good vacuum tightness at all interfaces. Good results were achieved with an additional surface finish by use of a coating. Both, vacuum tightness and geometrical tolerances were strongly improved.

For the curing process of the thin-walled boom half-shells an autoclave is not inevitably necessary. A good laminate quality was also achieved by vacuum bag processing inside a simple oven. For manufacturing studies, training purposes, and prototypes a bake-out tent was therefore installed. By use of this production facility it is possible to manufacture a complete deployable boom at

own internal facilities without external resources (Fig. 6). Since autoclaves are only available up to a certain length, the modular vacuum bag technology is an important economical alternative to produce very long booms. The qualification of the production facility and processes is, nevertheless, necessary. Meanwhile, first 14 m long boom shells were successfully produced with this new technology. The next process step after curing is the adhesive bonding process. The half-shells are bonded at the even flanges together. At this process step the exact positioning, in particular at large boom length, and the compliance with the process parameters are very important for a good boom quality.

### VERIFICATION

The boom design is based on a conventional CFRP technology in which extremely thin, unidirectional prepreps are used. During the material screening activities a number of potential carbon-fibre prepreps were investigated (Fig. 7). A Toray T300/2500 prepreg was chosen as technical baseline. Because this material has not been qualified for application in space up to now, considerable effort was made to prove its suitability and structural integrity for the mission goals in an in-orbit demonstration phase. The following tests were carried out within the material examinations so far:

- **static tension tests:** conventional material research under normal ambient conditions to determine the CFRP material stiffness and strength,
- **outgassing tests ECSS-Q-70-02A:** investigations with regard to the TML (Total Mass Loss) and CV-CM rates (Collected Volatile Condensable Material),

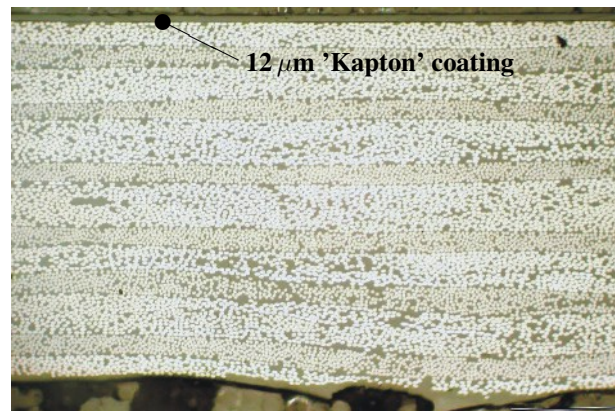


Fig. 7: Microimage during the material screening of a thin-walled 18-layered CFRP laminate (Bryte T300/EX-1522). Thickness 0.7 mm, 12  $\mu\text{m}$  Kapton coating applied.

- **thermal/vacuum aging tests ECSS-Q-70-04A:** visual inspection of thermally aged coupons; afterwards tension test in nominal boom longitudinal direction within a temperature range of  $[-196^{\circ}\text{C}; +100^{\circ}\text{C}]$ .

The stiffness and strength tests serve to control the theoretical assumptions, and very good conformity with the theoretical expectations could be determined. The outgassing tests were passed and the thermally aged samples were visually inspected and no damage could be determined. Tension tests in the nominal boom longitudinal direction were conducted after thermal aging at temperature intervals of  $[-100^{\circ}\text{C}; +100^{\circ}\text{C}]$ . It was even possible to realize a tension test at  $-196^{\circ}\text{C}$  as a random sampling. The measured CFRP stiffness and strengths do not lead to any conclusions regarding the degradation of the material properties in the researched temperature intervals that would come as a result of thermal aging.

Coated and un-coated boom sections were exposed to a one-sided radiation environment of  $1400\text{ W/m}^2$  ( $\sim 1\text{ AU}$ ) in the solar simulator at the DLR. A comparison of the transient temperature runs shows that the coating measures lower the temperature level considerably and the differences between the sides of the boom exposed to the sun and those opposite to it are less than those of the un-coated ones.

Full-scale bending tests and eigenfrequency measurements in cantilever configuration were defined on boom segments to verify the boom stiffness and buckling loads. Some of these tests were conducted under the influence of the additional thermal load of solar radiation on one side, as in the case in an application in Earth orbit. The temperature distribution was set due to a theoretical computation of up to  $100^{\circ}\text{C}$  on the compression-loaded side nearby the boom root by use of a single-sided radiator. The bending behavior expected to take place in accordance with theoretical buckling examinations could be generally confirmed. Load case  $M_x$  led to a sudden collapse after it reached the buckling limit. However, the booms behaved much more tolerantly at bending  $M_y$  and overcritical post-buckling areas were formed which means that further load increase was possible even after buckling occurs

#### CFRP booms: bending test results

buckling moments	[Nm]	$\hat{\sigma}_M$	$s$
... without thermal loading:	$M_{x,cr}$	83.9	3.14
	$M_{y,cr}$	51.5	3.51
... with thermal loading:	$M_{x,cr,t}$	76.9	1.25
	$M_{y,cr,t}$	42.6	2.66

Table 1: Engineering test of the buckling moments on 2 m long segments[7]: mean values  $\hat{\sigma}_M$  and standard deviations  $s$ ; the boom sections were partially heated up to a temperature level of approximately  $+100^{\circ}\text{C}$  nearby the boom root.

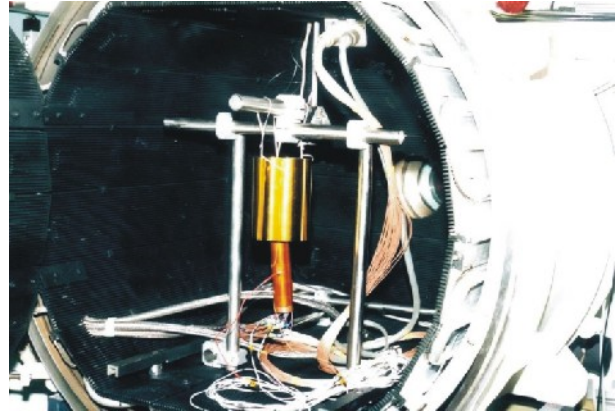


Fig. 8: Development testing on a coated boom section within the solar simulator chamber of the DLR. Structural bending test with 14 m long Solar Sail booms.

[7]. A good agreement with the theoretical expectations could also be determined for the buckling loads as well. Influence of the one-sided irradiation can only be determined on the buckling loads. The degradation effect on the critical buckling moments is significant (Tab. 1), yet an influence on the boom stiffness can not be identified. During the test the booms were loaded several times within the overcritical post-buckling area. Even a boom that was damaged on purpose was able to bear 92 % of the buckling load before it was damaged without losing a significant amount of stiffness. This clearly shows that the boom design is very damage tolerant.

During the mechanical tests problems came up which are strongly connected to the thin-walled CFRP shell structure's characteristic: the homogenous and rigid introduction of forces proved to be particularly difficult; the excellent boom performance therefore depends also on a proper interface design having enough stiffness itself. Although the bending stiffness  $EI_y$  with  $5308\text{ Nm}^2$  ( $s = \pm 109\text{ Nm}^2$ ) and  $5256\text{ Nm}^2$  ( $s = \pm 96\text{ Nm}^2$ ) in case of additional thermal loading is well within the expected range, yielding effects could be measured particularly at

bending about the  $x$ -axis. These degradations can be contributed to the performance of the boom clamping device, which was applied to the boom root during the cantilever tests. Nevertheless, they give an important feedback to the interface requirements.

### ADAPTIVE MEASURES

Large and extremely lightweight space deployable systems show very small natural frequencies. For a 40 m x 40 m version of the Solar Sail application the first natural frequency lays about 0.07 Hz. In combination with very low damping rates, large oscillation amplitudes and very long decay times arise (Fig. 9). The development of control systems, which are able to control and maneuver very low frequency systems, represents one of the most important future challenges in the design and operation of huge Gossamer structures. The specific influence on dynamic properties is therefore an important approach that extends the application spectrum of flexible deployable systems. The extreme requirements connected with it initiate the development of an innovative control strategy: smart structures with sensors and actuators that can change their geometrical shape and physical characteristic actively and adaptively.

The design of a Linear Quadratic Regulator (LQR) for the compensation of the dynamic behavior pursues to maintain the amplitude of the first excited mode of vibration small and to contribute to the stability under operational events. This active measure was implemented by using two PZT (=lead-zirconate-titanate) ceramics as actuators and one as a strain sensor. This design procedure was tested on a shortened sample of approximately 2 m length (Fig. 10).

Some experimental investigations on active suppression of vibrations in small structures using piezoelectric actuators have been reported in [3]. Some relatively larger scale experiments have been conducted using Jet Thrusters and Piezoactuators [5]. Different control strategies were invoked by the reported experimental studies, which included simple velocity feedback, simple adaptive feed-forward techniques, and modal feedback control using a set of spectral filters. Other analytical studies of active vibration control in elastic beams have been reported in [6].



Fig. 10: Test stand with the adaptive boom supported in cantilever form (length approx. 2 m).

State Space Model

### State Space Model

The pole locations for the flexible structure in this research are estimated from the non-parametric transfer functions of the system by using a frequency domain subspace identification technique. Figure 11 shows a sketch of the PZT actuated structure. As shown in the figure, the system has two PZT actuators located nearby the root of the boom, which generate the momentum to actuate the whole structure. The boom is excited by a sine sweep changing from 1 to 50 Hz for a period of 15 seconds. The sine sweep is produced by a signal generator, amplified, and sent to each of the PZT actuators separately. The signal from the PZT sensor is filtered using a 50 Hz fourth-order Butterworth filter and sent to a computer using a real-time data acquisition and control system at a sampling

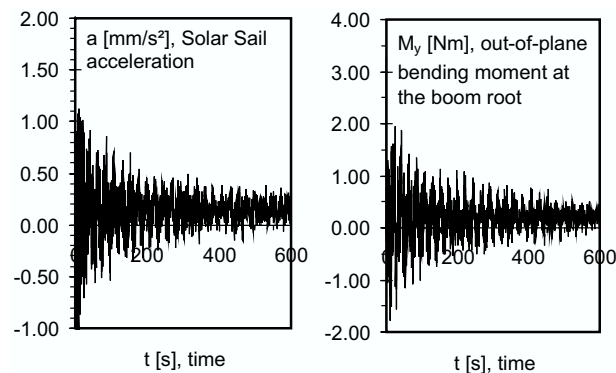


Fig. 9: Transient Solar Sail analysis of an acceleration maneuver out of Earth orbit (40 m x 40 m version). Rigid body acceleration and boom root loading [7].

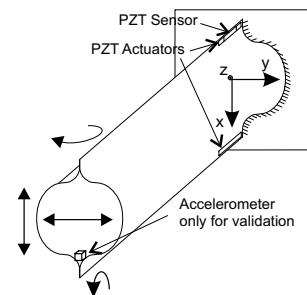


Fig. 11: Schematic representation of the bending oscillation experiment with adaptive measure.

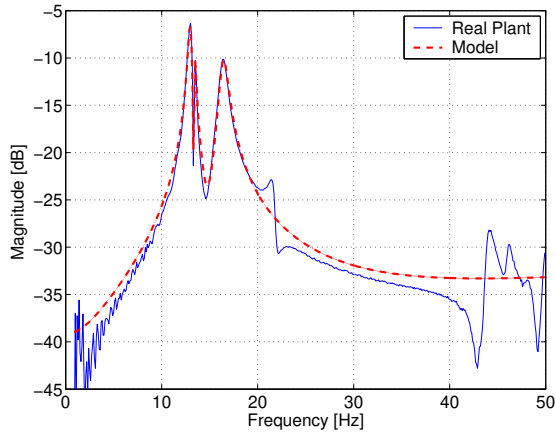


Fig. 12: Measured and modeled frequency response during bending oscillations along  $x$ -direction.

frequency of 1000 Hz.

The estimation of the frequency responses of the input-output measurements is realized by the Matlab command *tfe* using the spectral analysis technique based on Welch method. The state space models of the two-input, one-output piezoelectric sensor-actuator array system are identified over a bandwidth from 10 to 20 Hz. The software used for the system identification is SmartID of the company Active Control eXpert Inc.

A state space realization including the first vibration mode is

$$\begin{aligned} \dot{x} &= \mathbf{A}x + \mathbf{B}u \quad \text{and} \\ y &= \mathbf{C}x + \mathbf{D}u \end{aligned} \quad (1)$$

whereby  $\mathbf{A}$ ,  $\mathbf{B}$ ,  $\mathbf{C}$ , and  $\mathbf{D}$  represent the state space matrices. The dimensions of the matrices are  $n \times n$ ,  $n \times 2$ ,  $1 \times n$ , and  $1 \times 2$ , respectively. The order of the system is  $n = 8$ . The vectors  $x$ ,  $u$ , and  $y$  describe in each case the state vector, the input vector, and the output vector. This state space representation contains the first two modes along the  $x$ - and  $y$ -direction. The comparison between measured and modeled frequency responses represented in Figure 12 shows a very good correspondence in the relevant bandwidth between 10 Hz and 20 Hz.

### Controller Design

A feedback control law for suppressing simultaneously vibrations along the  $x$ - and  $y$ -directions will be based on the model represented by Equation 1. To validate

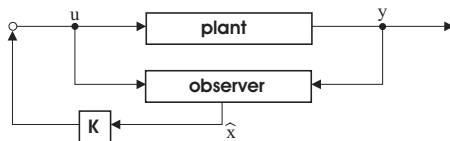


Fig. 13: Applied control technique: feedback with observer.

the identified model using the frequency domain, a high-performance controller is designed for the experimental flexible structure using the LQR control design framework.

A block diagram formulation of the control problem is shown in Figure 13. Because the system states are not directly measurable, a state observer will be utilized to estimate the states of the controlled system. The interconnection of the estimator is also represented in the Figure 13. The vector  $\hat{x}$  and the matrix  $\mathbf{K}$  represent the estimated state and the matrix gain of the observer, respectively.

The main objective is the reduction of the bending vibration during an external excitation at the boom's base. In order to achieve this objective, a strain signal is considered in the control design and two actuators at the base are used. The relevant bandwidth is between 10 and 20 Hz (63 and 126 rad/s). It contains the first two bending modes of the boom.

### Experimental Validation

Experiments have been conducted using the configuration shown in the Figure 10. The excitation for the control experiment was generated with an electrodynamic sha-

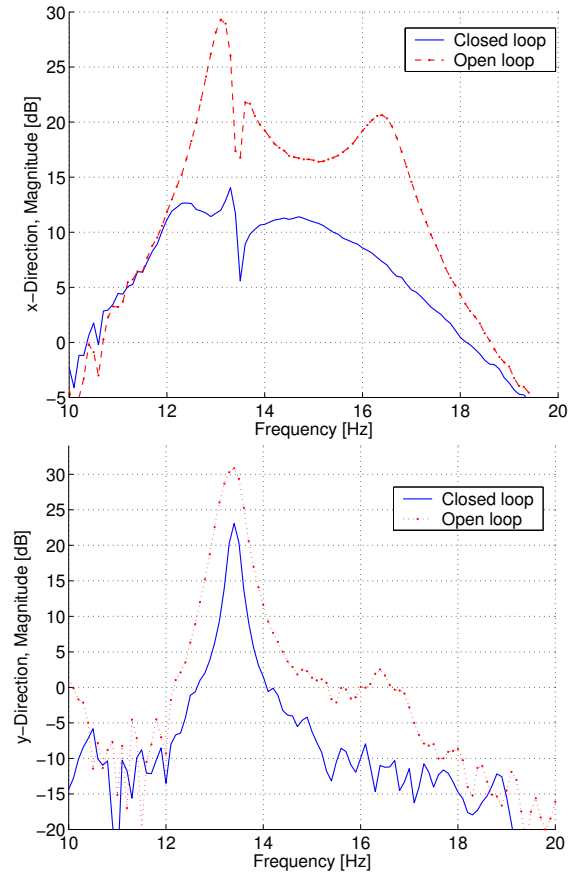


Fig. 14: Frequency responses with open and closed loop along  $x$ - and  $y$ -direction.



ker using a band-limited (10 to 25 Hz) sweep signal to drive the structure. The synthesized controller of the last section was modeled and implemented using a DSPACE system with a sampling frequency of 1 kHz. Figure 14 shows the comparisons of the open loop and closed loop frequency responses of the  $x$ - and  $y$ -directions, respectively, measured with an accelerometer at the tip of the boom. The test data also show that the damping controller is most effective in attenuating the mode vibration of the boom along the  $x$ -direction by about 15 dB, but is less effective for suppressing the modes vibration along the  $y$ -direction by about 7 dB because of the inconvenient position of the PZT ceramics in that case.

Basically the suitability of the method for the improvement of the dynamic behavior of large and flexible systems could be successfully demonstrated. However, the question of the scalability remains open, since this method was only tested on a short and stiff boom section compared to a potential application.

### APPLICATION AND OUTLOOK

Ultra-light, deployable structures are going to be fundamental components for a great number of potential space missions. Present and future applications are

- very long, deployable booms (gravity gradient, magnetometer, etc.),
- large, flexible solar arrays and membrane antennas,
- deployable reflectors,
- sunshades,
- solar space power systems,
- and Solar Sails.

From the engineering point of view, the requirements which are connected to the Solar Sail application mean an extreme challenge for the designers. They stand representatively for a number of general exercises that need to be worked out during the design of future large-scale and ultra-light deployable structures.

The innovative propulsion concept of the impulse transfer of solar photons onto a reflecting surface is used in Solar Sail concepts. Since the source of the propulsion does not have to be carried on board as is the case with conventional methods but is available in almost unlimited quantities in space, Solar Sails provide an interesting alternative to chemical propulsion methods especially for long-term missions that have a high demand for energy. The available thrust, however, is extremely small due to the very low mass of the reflected photons. A significant change in orbit energy can only be reached after a certain duration of the mission as a result of the continuous effect of acceleration or deceleration, respectively.



Fig. 15: Solar Sail Phase 0 – on-ground demonstration : Functional test with 14 m long deployable booms within the scope of the ESA/DLR Solar Sail technology demonstration. Gravity compensation for the boom assembly deployment was achieved by remote-controlled Helium balloons.

Because of the tremendous engineering challenges they have faced up to now, Solar Sail concepts have not yet advanced beyond theoretical design studies and a few functional breadboard models. Extreme lightweight construction, the development and verification of safe deployment concepts for large Gossamer structures, the realization of the long-term stability of the applied materials in the space environment, and finally the development of control concepts and mission analysis are important tasks that must be taken on in preparation of a first Solar Sail mission.

The acceleration of a Solar Sail results from the efficiency of the sail  $\eta$ , radiation pressure  $p_S$ , and the ratio of the entire mass of the spacecraft and the reflecting surface  $\sigma$  according to  $a = \eta p_S / \sigma$ . The entire Solar Sail assembly loading  $\sigma$  therefore has to be very small for an optimal acceleration. The degree of effectiveness  $\eta$  essentially depends on the optical properties of the sail and its homogenous tension and orientation. Too much tension in the sail, however, can lead to an excessive formation of wrinkles on the sail's surface and therefore has a negative influence on the degree of effectiveness. In addition, high tension forces require correspondingly massive support structures whose contribution to the mass budget can have a negative influence on the acceleration. Analyses on mid-term Solar Sail space missions estimate the necessary entire assembly loading to at least  $\sigma = 10 \dots 20 \text{ g/m}^2$  and sail sizes up to 125 m x 125 m [4]. These values clearly show the enormous challenges that engineers are faced with: new types of technologies have to be developed that facilitate the safe deployment of Gossamer structures in space; in addition, the deployment structure has to be extremely light and transportable within a very small volume on conventional launchers. At the same time, the ap-

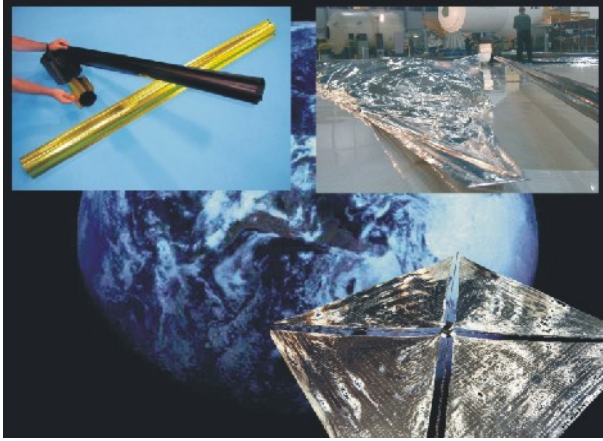


Fig. 16: Solar Sail Phase 1 – Earth orbit deployment demonstration: ESA and DLR are planning the demonstration in a joint effort. The DLR Institute of Structural Mechanics is involved by the hardware contribution of deployable CFRP booms and ultra-thin sail segments.

plied ultra-light structures have to prove their long-term stability in extremely different environments. A further challenge is the realization of a control concept that is able to safely manoeuvre large, flexible appendages with little energy expenditure and over long periods of time.

Within the scope of a Solar Sail technology demonstration ESA and DLR are developing further key technologies based on a successful on-ground functional test of a breadboard model (Fig. 15). The concept entails a square sail configuration that is mounted by four deployable CFRP booms, which are axially loaded in the deployed configuration by the sail tension forces. A central deployment module, which is also made by use of CFRP technologies, contains the boom assembly and the four triangular sail segments in a stowed configuration. Space qualification of the lightweight deployment concept is planned to be proved by an in-orbit verification of a 20 m x 20 m structure (Fig. 16). However, this deployment test does not yet aim at a real Solar Sail flight mission. It rather serves the validation of the deployment concept for huge membrane structures under space conditions.

The mass budget of a 40 m x 40 m Solar Sail, which would be technologically feasibly from today's point of

case study Solar Sail Phase 2: mass budget					
sub-sys.:	sail	booms	module	payl.	$\Sigma$
m [kg]:	14.9	11.4	46.8	10.0	83.1
$\sigma$ [g/m <sup>2</sup> ]:	10.6	8.1	33.4	7.1	59.4

Table 2: Estimation of the mass budget and the sub-system assembly loadings of a 40 m x 40 m Solar Sail including payload; sail: 1400 m<sup>2</sup> Kapton (7.5  $\mu$ m); booms: 4 x 28 m deployable CFRP booms (100 g/m).

view, is assessed in Table 2. The estimation is based on a specific boom mass of 100 g/m and sail segments which are made of a conventional 7.5  $\mu$ m Kapton film. It becomes apparent that both of these components have already a mutual assembly loading of approximately 18.7 g/m<sup>2</sup> compared with the sailcraft loading requirement of  $\sigma = 10 \dots 20$  g/m<sup>2</sup>, which comes from the flight mission analysis side. If additional masses are assumed for the deployment mechanisms and the payload, the necessity for further mass reductions will become even more apparent. Considering a 10 kg payload and a corresponding mass for the deployment module a sailcraft assembly loading of approximately 60 g/m<sup>2</sup> results.

The application of the detailed boom analysis to a system weight optimization is depicted in Figure 17 by the investigation of the boom assembly's margin of safety for an exemplary load case. Such analyses will pave the way for the exploration of further mass saving potentials. For the design of huge and flexible membrane structures two general questions will be of utmost significance which clearly affect the lightweight philosophy of the system:

I: **How great is the necessary membrane tension?** It must be big enough so that the membrane remains even under loading and that the sail is optimally effective. However, sail tensions that are too great can negatively influence the degree of effectiveness due to the formation of wrinkles. In addition, the support structure (booms) must be designed more stiffly and heavily. The reduction in the film thickness is very important since, under the assumption of a minimal sail tension that has to be maintained, the reduced thickness has a direct effect on the mass of the sail as well as on the design load of the support structure and therefore its mass. The determination of the optimal sail tension results from the optimization of the Solar Sail acceleration. Since the sail tension has an influence on the degree of effectiveness as well as on the mass budget, the lightest Solar Sail design does not necessarily also mean a maximization of the acceleration.

II: **What is the minimum system stiffness that must be maintained?** Mass optimizations such as those presented here inevitably lead to very flexible structures that border very closely on the static stability limit. As a result, the eigenfrequencies are extremely low and the oscillation amplitudes and decay times are very high due to low damping rates (Fig. 9). Requirements for the system stiffness in the form of minimal eigenfrequencies that have to be maintained or tolerable, dynamic oscillations like those that would have to be derived from an analysis of the manoeuvrability of suitable control concepts of a concrete design are presently not available.

Among these fundamental questions mass saving potential exploration concerns also the design of every sub-

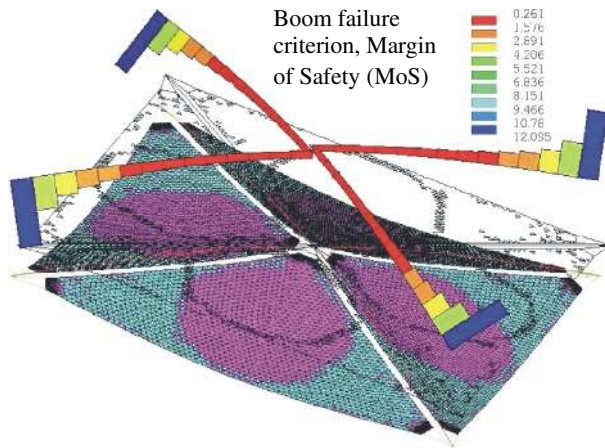


Fig. 17: Preparatory work for *Solar Sail Phase 2 – Earth orbit flight demonstration*: Lightweight optimization at system level. Case study of a 40 m x 40 m version with an assembly loading of  $\sigma \approx 60 \text{ g/m}^2$ . Load case 'air drag' at 300 km low Earth orbit. Application of a boom failure criterion [7].

system. A reduction in the mass of the sails can primarily be achieved by a reduction in the thickness. The CP1 films (clear polyimide) developed at NASA and distributed by SRS Technologies are available at thickness down to  $5 \mu\text{m}$  and further reductions are being pursued. Verifying the long-term stability of the coating is one of the main tasks during the development of the sail. In addition to the use of stiffer fibre systems and types of laminate, it is expected that mass reductions can be achieved in the deployable booms by means of a tapered design over the boom length. The assessment of the margins of safety depicted in Figure 17 makes it clear that the load is not homogeneously distributed over the boom lengths. The bending moments that are particularly important for the design become increasingly smaller the closer they get to the free boom tips. A particular strong point of the boom concept is scalability during the design, analysis, and manufacture that can be used in accordance with the lightweight philosophy of the design. It was not yet put into practice in the past for cost reasons. As far as the potential payload is concerned, miniaturization trends can contribute to a further reduction in the mass of a Solar Sail spacecraft. 'Picosatellites' that weigh less than 1 kg are based on technological developments in the field of microelectronics and micromechanics. The greatest saving potential, however, can be expected in the deployment technology. Ultra-lightweight deployment strategies that do completely or partially make use of the stowed deformation energy for the self-deployment could be interesting alternatives to existing concepts (Fig. 2). The jettison of unnecessary parts and mechanisms after deployment is a very effective method of saving mass as well. However, the risk of collision must be very closely analyzed at the start out of Earth orbit. Finally, the rigging of the

booms with a system made of tethers in accordance with classical lightweight philosophy standards is very effective since, in the ideal case, the structure only has to carry tension and compression loads, and bending moments are avoided. However, rigging concepts entail a great deal of risks during deployment at zero gravity, making their use for automatic deployment difficult.

From an engineering point of view, the requirement for an overall Solar Sail assembly loading of  $\sigma = 10 \dots 20 \text{ g/m}^2$  still poses enormous challenges. Yet, based on the design concepts available today as well as trends that have already been introduced, the development of an ultra-light deployment technology as a necessary prerequisite for a Solar Sail propulsion concept can be viewed as positive. Nonetheless, a lot of necessary development work still needs to be carried out before solar sailing takes place by entering Phase 3, the first space flight mission.

## LITERATURE

- [1] S. Lascar et. al. ESA space technology - harmonisation and strategy. Bulletin 112, ESA, Nov 2002.
- [2] L. Herbeck, M. Eiden, M. Leipold, C. Sickinger, and W. Unckenbold. Development and test of deployable ultra-lightweight CFRP booms for a Solar Sail. In *Proc. European Conf. on Spacecraft Structures, Materials and Mechanical Testing*, pages 107–112, ESTEC, Noordwijk, The Netherlands, 2000.
- [3] Joseph J. Hollkamp. Multimodal passive vibration suppression with piezoelectric materials and resonant shunts. *Journal of Intelligent Material Systems and Structures*, Vol. 5, January, 1994.
- [4] M. Leipold, E. Pfeiffer, P. Groepper, M. Eiden, W. Seboldt, L. Herbeck, and W. Unckenbold. Solar Sail technology for advanced space science missions. In *52th International Astronautical Congress*, Toulouse, France, Oct 1–5 2001. IAF-01-S.6.10.
- [5] A. Locatelli, F. Casella, and N. Schiavoni. Modeling and control for vibration suppression in a large flexible structure with jet thrusters and piezoactuators. *Transactions on Control Systems Technology*, 10(4), July 2002.
- [6] A. Preumont, A. Francois, P. De Man, and V. Piefort. Spatial filters in structural control. *Journal of Sound and Vibration*, 26(5):61–79, 2002.
- [7] C. Sickinger, L. Herbeck, and E. Breitbach. Structural engineering on deployable CFRP booms for a solar propelled sailcraft. In *54th International Astronautical Congress*, Bremen, Germany, Sep 29 – Oct 3 2003. IAC-03-I.4.05.